RSC Advances

ROYAL SOCIETY OF CHEMISTRY

www.rsc.org/advances

Fabricating conductive poly(ethylene terephthalate) nonwoven fabrics by using aqueous dispersion of reduced graphene oxides as sheet dyestuffs

Xin Liu[†], Zongyi Qin[†,*], Zhenjun Dou[†], Na Liu[†], Long Chen[†,*] and Meifang Zhu[†]

[†] *State Key Laboratory for Modification of Chemical Fibers and Polymer Materials, College of Material Science and Engineering, Donghua University, Shanghai 201620, China*

[*] *Address correspondence to phqin@dhu.edu.cn*

Abstract

A simple one–step dyeing–like approach was presented for fabricating conductive poly(ethylene terephthalate) (PET) nonwoven fabrics by using reduced graphene oxides (rGOs) as sheet dyestuffs. By using polyurethane (PU) as a middle adhesive layer, the rGOs can be adsorbed and well immobilized on the surface of PET fabrics due to strong attraction between two adjacent components. As a result, conductive fabrics with high structural stability were successfully prepared in aqueous dispersion of the rGOs. The as–prepared composite fabrics were characterized using scanning electron microscopy, Fournier transform infrared spectroscopy, Raman spectroscopy, and thermogravity analysis. The effects of the weight fraction of the rGOs on morphologies, structures and electrical properties of the composite fabrics were discussed. These composite fabrics exhibited a rather low electrical percolation threshold due to the homogeneous coverage of graphene sheets on the surface of PET nonwoven fabrics, and the highest conductivity was about 2.0×10^{-5} S/sq, ensuring the feasibility to manufacture efficient heating elements. Importantly, direct use of aqueous dispersion of the rGOs in dyeing would open new possibilities for massive production of graphene–based innovative fabrics.

Keywords: Conductive nonwoven fabrics, Poly(ethylene terephthalate), Reduced graphene oxide, Percolation transport, Thermal generation

1. Introduction

The importance of conductive textiles by integrating electronic functionality to the textile structures has been increasing because their various applications in many fields of activity, like possible applications in the areas of smart and e–textiles, chemical sensing, wearable electronics, energy conversion and storage[1-4]. Potential application would also be expected as biomedical devices, especially used as heating element in medical fields such as electrotherapy treatment, and medical blanket for maintaining the body temperature of the patients[5]. The conductive textiles are textile materials combined with electrical materials through different methods such as polymerization, metal wire inserting and coating techniques[1,6,7]. Coating techniques have been becoming attractive in the field of conductive textile, because textile materials with large surface area posses several advantages over conventional materials such as high flexibility and mechanical properties, making them good light–weight substrates to deposit some functional materials for different applications. Moreover, the process of coatings is relatively simple, cheap and materials obtained maintain their mechanical properties, along with electrical properties[6-9].

Graphene as a promising versatile nanofiller for polymers, which is defined as a single layer of sp^2–bonded carbon atoms arranged in a honeycomb lattice, can be produced in large quantity at low cost by chemical conversion from graphite[1,10-12]. In particular, because it is highly conductive, large surface area, and bendable, graphene has been considered as an excellent candidate for flexible conductive platforms[13,14]. As an intermediate in the manufacture of graphene, graphene oxide (GO) has structural feature similar to common textile dyes, such as the presence of an abundant number of hydroxyl and carboxyl groups[10].

Thus their homogeneous colloidal suspensions can be easily obtained without the need for either polymeric or surfactant stabilizers, which are widely used for carbon blacks or carbon nanotubes[1,5,15,16]. An approach similar to common dyeing and finishing method has been performed for fabricating conductive fabrics by directly placing the fabrics such as polyarylate[17], cotton[6,7,18] and polyester[8,9] in a solution containing the GOs as dyestuffs. It should be pointed out that these works were performed in both aqueous and polar organic solvents without the need for introducing foreign stabilizers or chemical modification[12,19]. However, the GOs are electrically insulating materials due to their disrupted sp^2 bonding networks[12]. In order to obtain conductive fabric, further reduction of the GOs into reduced graphene oxides (rGOs) must be done at a relatively high temperature [10,20]. It is noted that rGOs consist of few–layer thick and electronically conductive graphitic sheets, which makes them suitable for synthesis of conducting nanocomposites[10,12]. Unlike perfect graphene sheets which tend to aggregate with each other and is hard to disperse in aqueous solution, rGOs with a considerable amount of sheet defects exhibit relatively stable in an aqueous dispersion, and have the versatility of being amenable to a range of solution processing techniques[19].

Poly(ethylene terephthalate) (PET) is one of the most widely used low–cost polymers due to its excellent thermal and chemical resistance and mechanical performance, and PET nonwoven fabrics as one of the most important fabrics. The above mentioned properties of PET film are encouraging for its application as structural material. Although local electrostatic interaction between graphene and PET occurred[21], these finishes did not withstand subsequent washing due to poor fixing of the graphene sheets on the textile surface. Assuring improved bonding of rGOs with textile surfaces not only increases the durability property, but also open

new possibilities for the massive production of graphene–based innovative fabrics. In this work, a low–cost approach of dyeing PET nonwoven fabrics would be presented by anchoring the rGOs on the surface of the fabrics in aqueous system.

2. Materials and methods

2.1 Preparation of aqueous dispersion of rGOs. The rGOs were obtained by chemical reduction of readily available exfoliated GOs with $N_2H_4 \bullet H_2O$, which were synthesized by a modified Hummers method[1,6]. In a typical treatment, 10.0 g of graphite and 7.5 g of $NaNO_3$ powder were added to 230 ml of cooled (0 °C) H_2SO_4 (98%). 30.0 g of $KMnO_4$ was added gradually with stirring at 35 °C for 45 min. Then 460 ml of distilled water was slowly added to the mixture. After 15 min, the reaction was terminated by adding 1400 ml of distilled water followed by 100 ml of 30 % H_2O_2 solution. Therefore, the GOs were obtained by washing the suspension with deionized water until the pH reached 7. Afterwards, 1.0 g GO was highly dispersed in 1000 ml deionized water, and subsequently 1 ml hydrazine hydrate was added. The reaction was kept at 98 ^{o}C with mechanical stirring for 1 h, and the black product was filtered with a Buchner funnel and washed with deionized water until the pH reached 7. Only a small fraction of the as–prepared rGOs were dried in the oven at 60 ^{o}C for 24 h for comparison, and most of them were dispersed again in deionized water under ultrasonication to prepare aqueous suspension containing the weight fraction of the rGOs ranging from 0.001 to 0.150 wt.%.

2.2 Preparation of conductive PET fabrics. PET nonwoven fabrics were firstly immersed into 0.1 wt.% PU in DMF at room temperature for 60 s. After drying, the fabrics

were washed with deionized water to remove residual DMF, and then dried in ambient conditions overnight. As shown in **Fig. 1**, the as–prepared composite fabrics were immersed in the above–mentioned aqueous suspension with a liquor ratio of 100:1. The fabric dyeing was carried out in a bath of ice and water under ultrasonication for 10 min. After dried at 80 ^{o}C in an oven overnight, dark–brown PET composite fabrics were obtained.

2.3 Apparatus. The morphologies of PET nonwoven fabrics and as–prepared composite fabrics were observed on a field emission scanning electron microcopy (FE–SEM) (S–3000N, Hitachi, Japan). The morphologies of the rGOs were observed on a NanoScope IV Multimode Atomic force Microscope (AFM) (Veeco, Santa Barbara, CA), equipped with an E scanner and NSC11/AIBS cantilevers (MikroMasch, Tallinn, Estonia). The samples were prepared by casting a heavily diluted aqueous rGO suspension on the surfaces of silicon chips. The images were obtained using the tapping mode at a scanning rate of 1 Hz, and the cantilever with a spring constant of 40 N/m was used.

Chemical structures were characterized on an attenuated total reflectance accessory of Fourier transform infrared (FT–IR) spectrometer (Nicolet 8700, American) and a micro–Raman spectrometer (inVia+Reflex, Renishaw, England). FT–IR spectra were obtained with a resolution of 4 cm^{-1}, scan number of 200 and the scan area from 400 to 4000 cm^{-1}. Raman spectra were recorded using the 532 nm line of an argon ion laser with 50 mW output power.

Thermal stabilities were tested by thermo–gravimetric analyzer (TG209F1, Netzsch, Germany) with a heating rate of 20 °C/min under a nitrogen atmosphere. Structural stabilities of the composite fabrics were evaluated by treating the fabrics in water under ultrasonication

with different powers, and stirring at different rotation rates, respectively.

Electrical measurements were carried out with the two–electrode method in case of applying voltage of 100 V by using an Insulation Resistance Meter (BH828, China). The dimension for the applied fabrics was 3×3 cm^2. Surface conductivity of the composite fabric was calculated using the equation, $\sigma=D/(R_s \cdot L)$, where D is the distance of two electrode, R_s the resistant of the sample, and L the width of the electrode. Heat generation characteristics were performed by using a DC power supply (WYJ, 3A, 30V). A thermometer was inserted to six fabric samples (5×5 cm^2) and positioned half way, and then the edges of the fabrics were regulated by two cramps and connected to the terminals of the power supply.

3. Results and discussion

3.1 Morphology. Using the dyeing–like process, the surfaces of PET nonwoven fabrics were covered successively with the rGOs at different weight fraction in aqueous dispersion. As shown in **Fig. 1**, the as–prepared black composite fabrics still kept excellent mechanical properties of PET nonwoven fabrics. Furthermore, AFM was used to evaluate the morphologies of the resultant rGOs. The apparent height for the observed rGOs with different geometric shapes was found to be around 3 nm as shown in **Fig. 1**, indicating that the rGO consisted of three–layer graphene sheets, and the width for most of the rGO was more than 10 micrometers. Due to partial removal of hydroxyl and carboxyl groups, rGOs are easily exfoliated in water forming stable colloidal dispersions. In order to achieve the uniform coverage of the rGOs on the surface of the fabrics, the preparation process was performed under ultrasonication. Herein, PET nonwoven fabrics were treated with PU solution in DMF

before dyeing, ensuring that the rGOs can be adsorbed and well immobilized on the surface of the PET fabrics due to strong attraction between two adjacent components[4,16,22-24]. If not, it is very easy to remove the rGOs from the surface of the fabrics through a simple washing procedure. Through a very thin PU adhesion layer, rGO functioned as sheet–shaped dyestuffs being firmly attached on the surfaces of multifilament years through the traditional dyeing approach.

SEM was used to observe the morphologies of the PET nonwoven fabrics and the resulting composite fabrics prepared in aqueous dispersion containing different rGO contents. There was almost no difference in the morphology and diameter for PET nonwoven fabrics before and after PU treatment. Furthermore, similar morphology can be found for low weight fraction of the rGOs as shown in **Fig. 2**, and it is difficult to identify whether efficient coverage of very thin sheets of the rGOs with two–dimensional forms on the surface of the fabrics. With the increasing of the rGO fraction, the colour of the fabrics turned from dark–brown to black, and some aggregates or the folds developed during the deposition process can be observed on the surface of the fabrics. Especially, a higher number of the rGO aggregates can be commonly observed at the intersection of the fibers for larger rGO fraction.

3.2 Percolation electrical transition. **Figure 3** displays the change in surface conductivity of the composite fabrics with the increasing of the weight fraction of the rGOs in aqueous dispersion. Generally, when the conductive nanofillers form a conductive network in an insulating matrix, the direct current electrical conductivity of the composites increases rapidly, and subsequently electrical percolation threshold of the composites can be measured. As shown in **Fig. 3**, the conductivity of the composites fabrics increases sharply once the rGO

fraction exceeded a threshold of about 0.0012 wt.%. At the nanofiller content about 0.010 wt.%, the conductivity of composites fabrics already satisfied the antistatic criterion (10^{-6} S/sq), which is about 8 orders of magnitude higher than that of PET fabrics (2.2×10^{-14} S/sq). Then the conductivity of composites fabrics continued to increase gradually with the increase of the nanofiller content, and reached to a saturation value of 2.0×10^{-5} S/sq when the rGO fraction reached to 0.080 wt.%, which is comparable with the value for the conductive polyester fabric (9.1×10^{-5} S/sq)[17]. It is worth noting that in contrast with one–step fabrication performed in this work, a further reduction was involved in the preparation of conductive polyester fabrics by using the GOs as dyestuffs, in which the GO–dyed fabrics were again immersed in an aqueous solution containing 0.5 wt.% sodium hydrosulfite at about 363 K for 30 min[17].

Furthermore, to better understand the formation of conducting pathways over the fabric, the inserts in **Fig. 3** give three different surface morphologies for the composite fabrics prepared at various rGO fractions in initial aqueous dispersion. At low rGO fraction, fewer folds appeared on relative smooth fabric surface as shown in **Fig. 3(I)**, implying that most deposited rGOs were presented in two–dimensional form. When the rGO fraction exceeded 0.001 wt.%, an abrupt increase in the conductivity of the composite fabrics occurred. With more rGOs deposited onto the surface of the fabrics, more folds could be found as shown in **Fig. 3(II)**. It is found that the irreversible agglomeration would take place for all rGO samples during the reduction process with the reason of their hydrophobicity[25]. These wrinkled and overlapped graphene sheets can link the individual graphene sheets effectively and carry a high current density, resulting in high electrical conductivity. These folded rGOs became

increasingly interconnected and finally formed a continuous conducting network as shown in **Fig. 3(III)**, and did not show an increase in conductivity with a further increase in the density of the conductive network.

The conductivity of the composites fabrics can be further rationalized in terms of modified classical percolation theory, $\sigma=\sigma_0(\varphi-\varphi_c)^t$, where σ represents the conductivity of the composite, φ is the rGO fraction, φ_c the percolation fraction, and t the critical exponent[12,23-26]. For a single percolation system, the critical exponent depends only on the dimensionality of the composites, and follows a power–law dependence of approximately 2 in a three–dimensional and 1~1.3 in a two–dimensional system[12,23,24]. Using the data in **Fig. 4**, t was estimated to be 1.35, indicating the presence of a two–dimensional conductive network on the surface of the composite fabrics. The electrical percolation threshold was about 0.0012 wt.%. Such a rather low electrical percolation threshold can be explained by the extraordinarily large specific surface area of graphene sheets and their homogeneous coverage of graphene sheets on the surface of PET nonwoven fabrics. However, due to only partial reduction of the GOs occurred under the mild condition, some oxygen–containing functional groups would still remain on the surface of rGOs, which resulted in low electrical conductivity.

3.3 Chemical structure. FT–IR and Raman spectra for rGO, PU, PET, PU–treated PET and the composite fabrics prepared in aqueous dispersion containing different rGO contents were given as shown in **Fig. 5(a) and (b)**, respectively. For the rGO, all the IR bands arising from oxidized groups were substantially reduced although they did not completely disappear as shown in **Fig. 5(a)**. For the rGOs, besides a band around 1533 cm^{-1} assigning to skeletal

vibration of graphene sheets[8], a band around 1723 cm^{-1} and a weak band around 1025 cm^{-1}, which mainly resulted from oxygen–containing groups at the edges of the rGOs[8,10], were attributed to stretching vibrations of C=O, and stretching vibrations of C–O, respectively. When the rGOs were deposited on PU–treated PET fabrics, no substantial variation was observed compared with the infrared spectra of pure PET fabric, but only a very slight decrease for the different bands of PET. In addition, the baseline shift caused by the rGOs became more obvious with the increase of the rGO content.

Similarly, it is difficult to identify the PU characteristic bands in the composite fabrics. Just as mentioned above, it is very necessary to treat PET nonwoven fabrics in the PU solution in DMF before dyeing. It is found that only a slight influence of the treatment time on the conductivity of the composite fabrics as the time exceeded 1 min. To avoid the damage of PET fabrics in DMF, it should be done within 1 min for preparing the PU–treated PET fabrics. This implies very thin PU layer would be formed on the surface of PET fabrics, which has almost no influence on the diameter of the fabrics observed by SEM images as mentioned previously. It has been demonstrated that strong interface adhesion can be achieved through the interaction between the carbonyl group of PET and –NH group of PU[27], and dipolar interactions or hydrogen bonding between oxygen–containing functional groups in rGO and PU[16,22]. However, the change in the infrared spectra of the composite fabrics induced by these interactions cannot be properly discerned, because both very thin PU and rGO layers were covered on the PET fabric surface.

Raman scattering is strongly sensitive to the electronic structure, and has proved to be an essential tool to characterize graphene–based materials[11,20.] As shown in **Fig. 5(b)**, the rGOs

exhibit a strong D and G band, and a weak and broad 2D band. G band corresponds to an E_{2g} mode of graphite which is related to the vibration of sp^2–bonded carbon atoms in a two–dimensional hexagonal lattice (at 1575 cm^{-1}), D band (at 1343 cm^{-1}) is caused by the defects and disorders in the hexagonal graphitic layers, while 2D band is attributed to a double–resonance process resulting in the production of two phonons with opposite momentum[6,11,28]. The D band, which is defect–related, appears as a strong band for a thick graphite sample with a large number of layers. The ratio (I_G/I_D) of the intensities of the G and D bands is related to the sheet thickness of few–layer graphene samples[11], and a relatively low intensity ratio between G peak and D peak reveals most of the oxygen-containing functional groups are removed and a more efficient reduction of the GOs[20,25]. For the rGOs used in this work, the ratio was about 0.84. According to the equation, $L_a=4.4(I_G/I_D)$[11], the rGO sheet thickness (L_a) was found to be 3.70 nm, which was consistent with that determined by AFM method. Moreover, similar to infrared spectral observations, all the characteristic bands for PET appeared in the spectra of the composite fabrics, but no obvious PU bands can be identified. In addition, with the increasing of the rGO fraction in the dispersion, the increase in the intensity for rGO bands can be noted, indicating more rGOs deposited on the surface of PET fabrics.

3.4 Structural Stability. **Figure 6(a)** shows TGA curves of rGO, PU, PET, PU–treated PET, and the composite fabrics prepared in aqueous dispersion containing the rGO content of 0.010, 0.030 and 0.080 wt.%, respectively. TGA curve of the rGOs exhibited slight weight loss below 100 ^oC, showing the removal of oxygen–containing functional groups as well as water content[25]. Furthermore, a weight loss stage appeared in TGA curve from 150 to 300 °C,

possibly due to loss of CO and CO_2 from decomposition of oxygen functional groups[28]. The initial decomposition temperature (T_0) and maximum decomposition temperature (T_{max}) for PET nonwoven fabric were about 380 and 450 ^oC, respectively. Compared with neat PET, the composite fabrics exhibited slight decrease of thermal stability, but being clearly superior to PU–treated PET fabric. Furthermore, the composite fabric for the rGO content of 0.030 wt.% shows the best thermal stability, and the highest T_{max} appeared for 0.080 wt.% among the composite fabrics. Usually, the weight fraction for the deposited rGOs can be estimated from TGA curves by analyzing the residual weight for different rGO fractions at high temperature. Unfortunately, the actual weight fraction of the rGOs could not be determined in a small error range due to extremely low rGO content on the surface of the fabrics.

It is important for the composite fabrics to ensure long–term structural and electrical stability in practical applications. To evaluate the structural stability, the composite fabrics prepared at the rGO content of 0.080 wt.% were respectively treated with deionized water under ultrasonication with different power, and washed with water in 40 ^oC through mechanical stirring at different speed. **Figure 6(b)** shows only slight change in the conductivity of the composite fabrics under ultrasonic irradiation with the power of 50 W. When the power was changed to 275 W, the relative change in the resistance increased roughly 5 fold, and then remained a stable stage after 5 cycles. **Figure 6(c)** displays the effect of the stirring speed on the relative change in the resistance. It is found that large change in the relative resistance occurred at high stirring speed before 5 times of water washing, and then remained almost unchanged. These tests demonstrated that such thin rGO–skin functions as electrically conductive layers had excellent adhesion, flexibility, and durability.

3.5 Heat generation. By controlling the weight fraction of the rGOs in aqueous dispersion, a wide range of electrical conductivity for the composite fabrics could be offered. It has been reported that the fabrics with 10^{-9} S/sq conductivity can be expected to be used as brushes in photocopying machines, and with 10^{-5} S/sq for anti–static clothing, and moreover, personal heating garments for generating sufficient heat to warm up the body under relatively low applied voltage[17]. **Figure 7** gives the electrothermal performances for the composite fabrics with the valid heating area of 5×5 cm^2 under ambient conditions. It is found that a corresponding exponential rise in temperatures over time until a steady–state temperature, which could get higher when a larger voltage was applied. For the composite fabrics prepared in aqueous dispersion containing 0.080 wt.% rGOs, a steady–state temperature of 59 °C can be reached in less than 30 min at 30 V. These results demonstrated the feasibility of fabricating efficiently heating element by using these composite fabrics for maintaining patient body temperature. What is more, the direct use of rGOs as sheet dyestuffs in aqueous dispersion opens new applications of nanotechnologies in fiber, fabrics or textile productions. For example, the interaction between graphene and metal oxide nanocrystals or conducting polymers provides the hybrids with additional properties, offering rich opportunities for the composite fabrics to tune the material structure and properties[11,13,14,29].

4. Conclusion

Conductive PET nonwoven fabrics were successively prepared through a conventional dyeing approach by utilizing rGOs in aqueous dispersion as sheet dyestuffs. High uniform coverage of the rGOs and structural stability of the composite fabrics were benefited from the

use of PU thin adhesion layer. By controlling the weight fraction of the rGOs in the initial aqueous dispersion, a wide range of electrical conductivity from 10^{-13} to 10^{-5} S/sq for the composite fabrics could be offered. With the increasing of the rGO fraction, a continuous interconnection network was formed over the surface of PET nonwoven fabrics with low percolation fraction of the rGOs. Moreover, the feasibility of the composite fabrics as efficient elements for thermal generation was demonstrated. Our findings make it possible to process graphene materials in high volume production using low−cost solution processing techniques for preparing flexible conductive textile. Possible practical application with the interconnected conductive networks as the functional elements for heat generation has been evaluated. What is more, flexible conductive platforms which can provide a support for metal oxide and conductive polymers can be manufactured at very low cost and integrated into smart textiles.

Acknowledgements

This work has been financially supported by National Natural Science Foundation of China (21274019), Fundamental Research Funds for the Central Universities (2232013A3-02), and Program for Changjiang Scholars and Innovative Research Team in University (IRT1221).

References

1 L. Hu , Y. Cui, *Energy Environ. Sci.*, 2012, **5**, 6423–6435.

2 C. Xiang, W. Lu, Y. Zhu, Z. Sun, Z. Yan, C. Hwang, J. M. Tour, *ACS Appl. Mater. Interfaces*, 2012, **4**, 131−136.

3 G. Yu, L. Hu, M. Vosgueritchian, H. Wang, X. Xie, J. R. McDonough, X. Cui, Y. Cui, Z. Bao, *Nano Lett.*, 2011, **11**, 2905–2911.

4 Z. Tai, X. Yan, Q. Xue, *J. Power. Sour.*, 2012, **213**, 350–357.

5 B. Fugetsu, E. Akiba, M. Hachiya, M. Endo, *Carbon*, 2009, **47**, 527–544.

6 W. Liu, X. Yan, J. Lang, C. Peng, Q. Xue, *J. Mater. Chem.*, 2012, **22**, 17245–17253.

7 L. Hu, M. Pasta, F. La Mantia, L. Cui, S. Jeong, H. D. Deshazer, J. K. Choi, S. M. Han, Y. Cui, *Nano Lett.,* 2010, **10**, 708-714.

8 J. Molina, J. Fernández, J. C. Inés, A. I. del Ríom, J. Bonastre, F. Cases, *Electrochim Acta*, 2013, **93**, 44–52.

9 J. Molina, J. Fernández, A. I. del Río, J. Bonastre, F. Cases, *Appl. Surf. Sci.*, 2013, **279**, 46–54.

10 S. Park, R. S. Ruoff, *Nat Nanotechnol*, 2009, **4**, 217–224.

11 C. N. R. Rao, K. Biswas, K. S. Subrahmanyam, A. Govindaraj, *J. Mater. Chem.*, 2009, **19**, 2457–2469.

12 S. Stankovich, D. A. Dikin, G. H. B. Dommett, K. M. Kohlhaas, E. J. Zimney, E. A. Stach, R. D. Piner, S. T. Nguyen, R. S. Ruoff, *Nature*, 2006, **442**, 282−286.

13 S. Cui, S. Mao, G. Lu, J. Chen, *J. Phys. Chem. Lett.*, 2013, **4**, 2441−2454.

14 I. V. Lightcap, P. V. Kamat, *Acc. Chem. Res.*, 2013, **46**, 2235–2243.

15 A. G. Goncalves, B. Jarrais, C. Pereira, J. Morgado, C. Freire, M. F. R. Pereira, *J. Mater. Sci.,* 2012, **47**, 5263–5275.

16 J. Gao, M. Hu, Y. Dong, R. K. Y. Li, *ACS Appl. Mater. Interfaces,* 2013, **5**, 7758–7764

17 B. Fugetsu, E. Sano, H. Yu, K. Mori, T. Tanaka, *Carbon*, 2010, **48**, 3340–3345.

18 M. Shateri–Khalilabad, M. E. Yazdanshenas, *Carbohydrate. Polym.*, 2013, **96**, 190–195.

19 D. Li, M. B. Müller, S. Gilje, R. B. Kaner, G. G. Wallace, *Nat. Nanotechnol.*, 2008, **3**, 101–105.

20 Y. Shen, S. Yang, P. Zhou, Q. Sun, P. Wang, L. Wan, J. Li, L. Chen, X.Wang, S. Ding, D. W. Zhang, *Carbon,* 2013, **62**, 157–164.

21 W. Park, S. Noh, M. Joo, T. Kim, W. Park, M. Jung, J. Moon, K. Park, *Appl. Phys. Lett.,* 2013, **103**, 033107–1–4.

22 N.Yousefi, M. M. Gudarzi, Q. Zheng, X. Lin, X. Shen, J. Jia, F. Sharif, J. K. Kim, *Composites: Part A*, 2013, **49**, 42–50.

23 N. Yousefi, M. M. Gudarzi, Q. Zheng, S. H. Aboutalebi, F. Sharif, J. K. Kim, *J. Mater. Chem.*, 2012, **22**, 12709–12717.

24 K. H. Liao, Y. Qian, C. W. Macosko, *Polymer*, 2012, **53**, 3756–3761.

25 S. Bai, X. Shen, G. Zhu, A. Yuan, J. Zhang, Z. Ji, D. Qiu, *Carbon*, 2013, **60**, 157–168.

26 H. Zhang, W. Zheng, Q. Yan, Y. Yang, J. Wang, Z. Lu, G. Ji, Z. Yu, *Polymer*, 2010, **51,** 1191–1196.

27 C. K.Samios, K. G. Gravalos, N. K. Kalfoglou, *Eur. Polym. J.*, 2000, **36**, 937–947.

28 J. Shen, T. Li, Y. Long, M. Shi, N. Li, M. Ye, *Carbon*, 2012, **50**, 2134–2140.

29 J. Zhu, M. Chen, Q. He, L. Shao, S. Wei, Z. Guo, *RSC Adv.*, 2013, **3**, 22790–22824.

Figure captions

Fig. 1 Schematic for the fabrication of rGO–coated PET nonwoven fabrics.

Fig. 2 SEM images of PET nonwoven fabric and the resulting composite fabrics prepared in aqueous dispersion containing different rGO contents. (a) PET nonwoven fabric; (b) 0.001 wt.%; (c) 0.010 wt.%; (d) 0.030 wt.%; (e) 0.080 wt.% and (f) 0.150 wt.%.

Fig. 3 Change on surface conductivities of the composite fabrics with the increasing of the weight fraction of the rGOs in the initial aqueous dispersion. The inserts display the SEM images of the composite fabrics prepared at the rGO fraction of 0.001 (b), 0.030 (c) and 0.080 wt.% (d), respectively.

Fig. 4 Linear fitting for percolation electrical transition occurred for the composite fabrics prepared in aqueous dispersion with the increasing of the rGO content.

Fig. 5 FT–IR (a) and Raman (b) spectra for rGOs, PU, PET nonwoven fabric, PU–treated fabric and the resulting composite fabrics prepared in aqueous dispersion containing different rGO contents.

Fig. 6 Evaluation of thermal (a) stability for the composite fabrics prepared in aqueous dispersion containing the rGO content of 0.010, 0.030 and 0.080 wt%, respectively, and structural stability (b and c) for the rGO content of 0.080 wt.%. (b) Ultrasonication; (c) Stirring.

Fig. 7 Time dependence of temperature for the composite fabrics prepared in aqueous dispersion containing the rGO content of 0.080 wt.%.

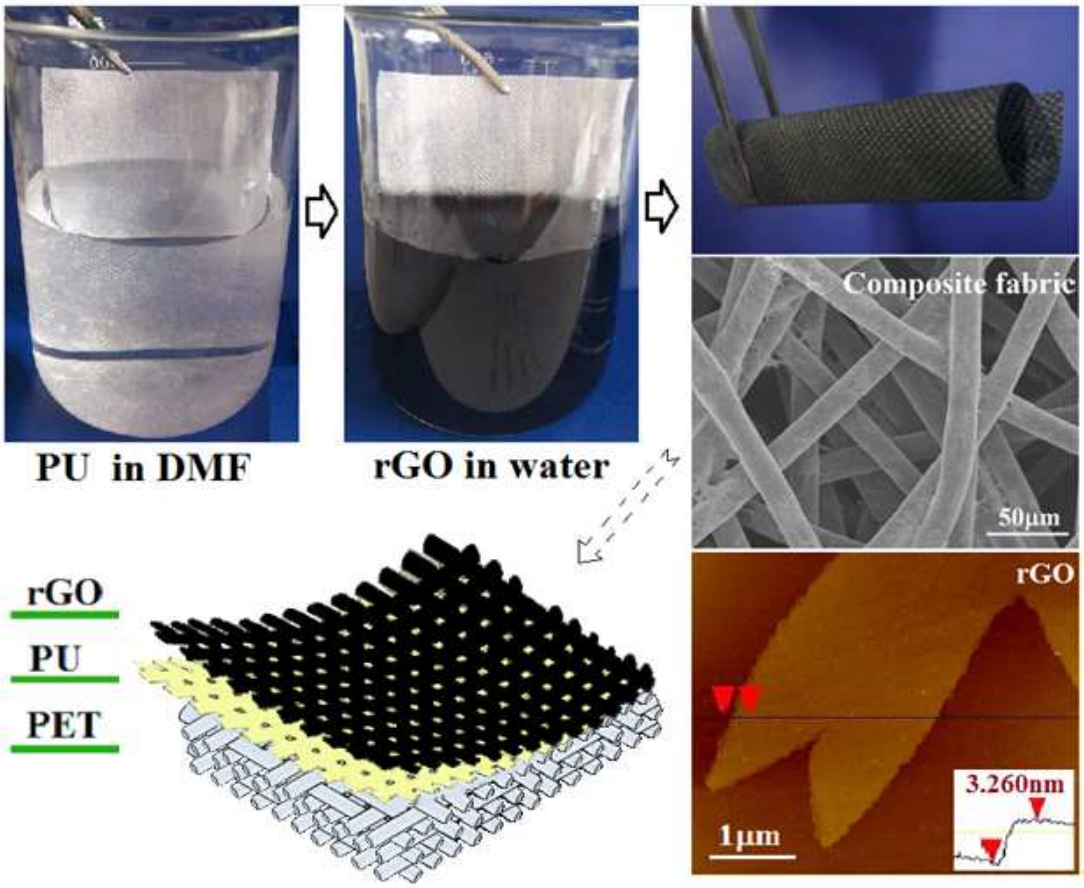

Fig. 1

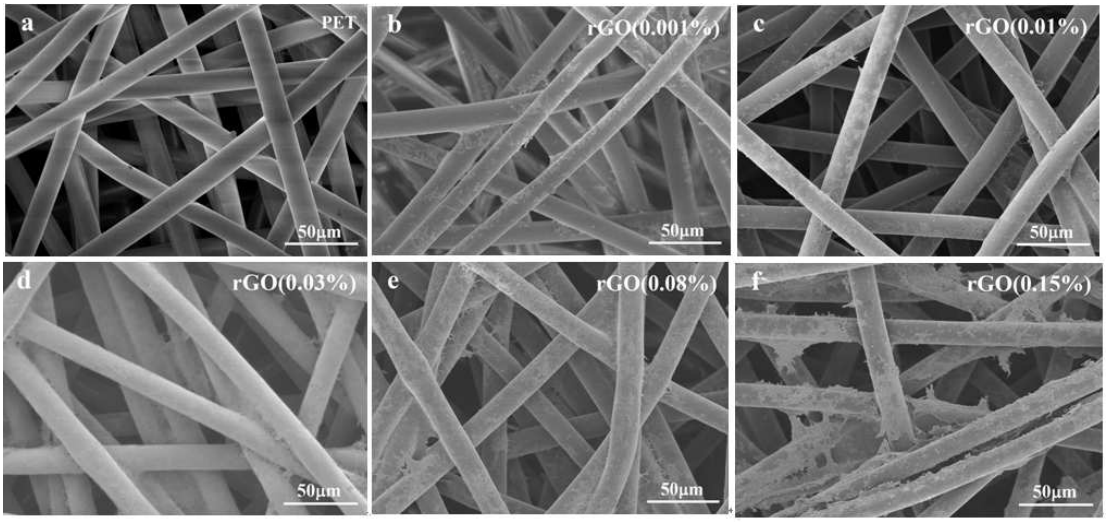

Fig. 2

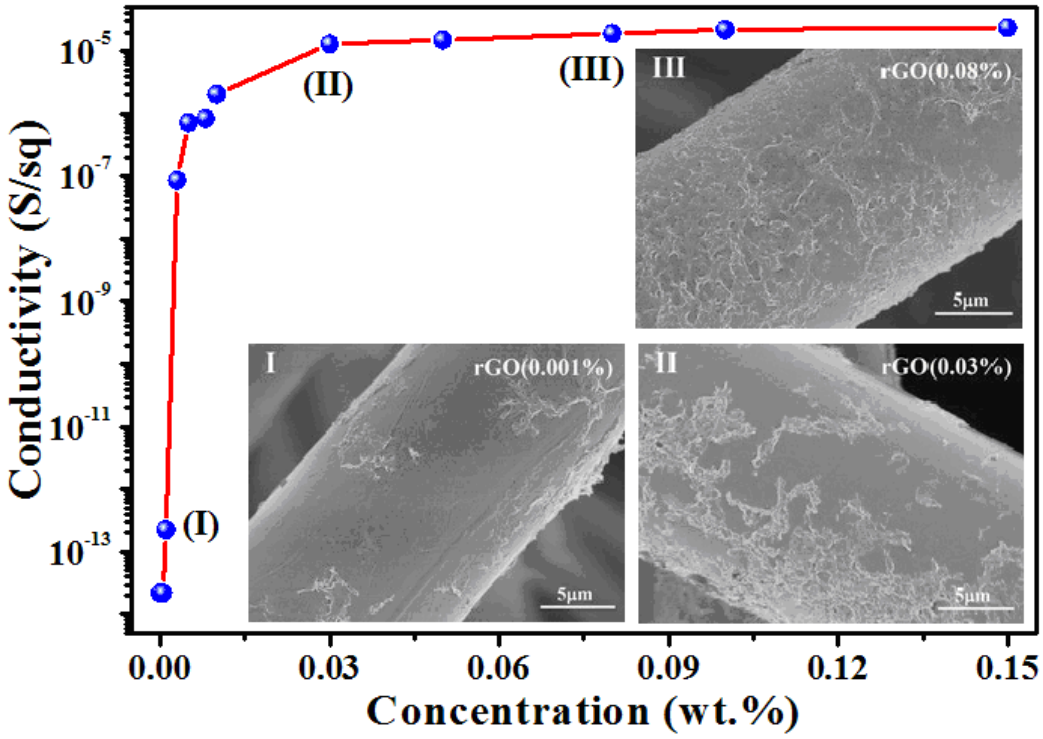

Fig. 3

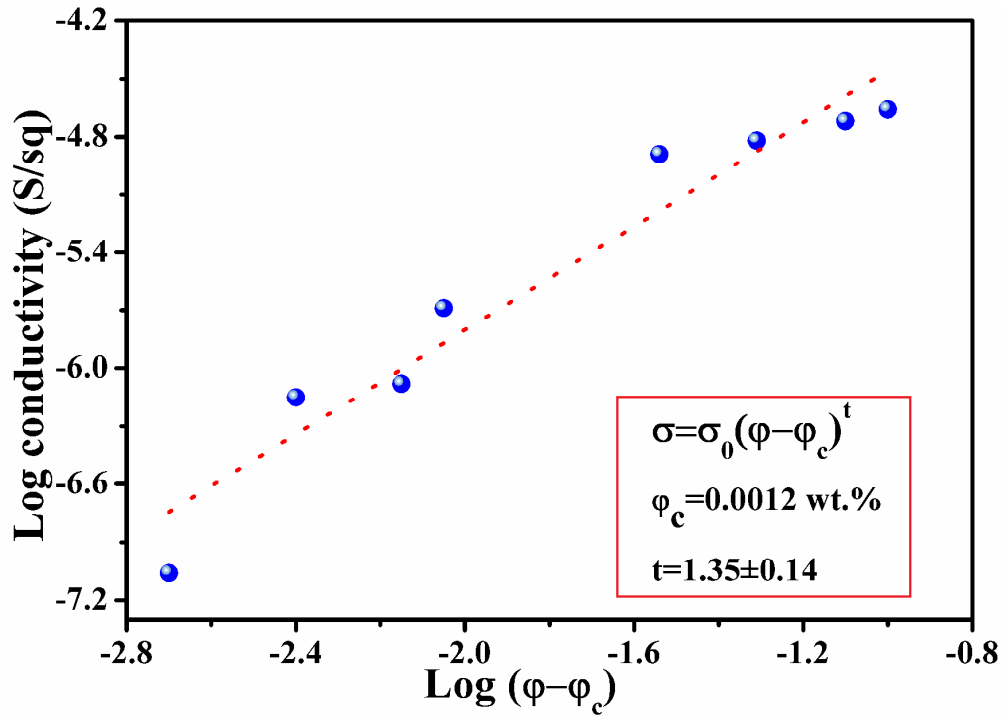

Fi.4

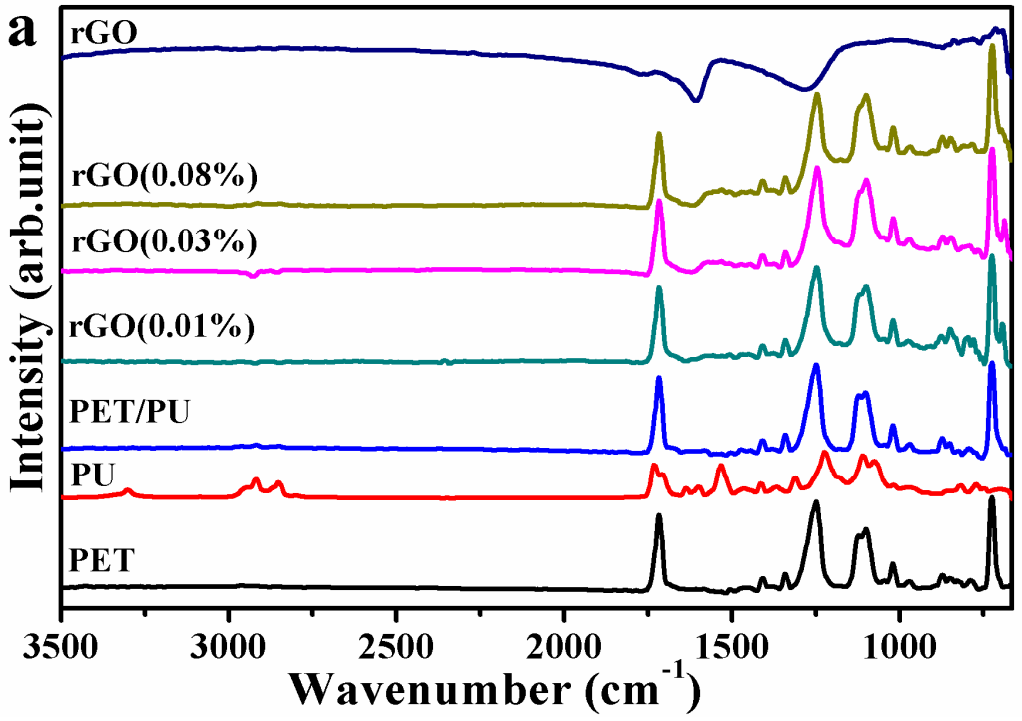

Fig. 5(a)

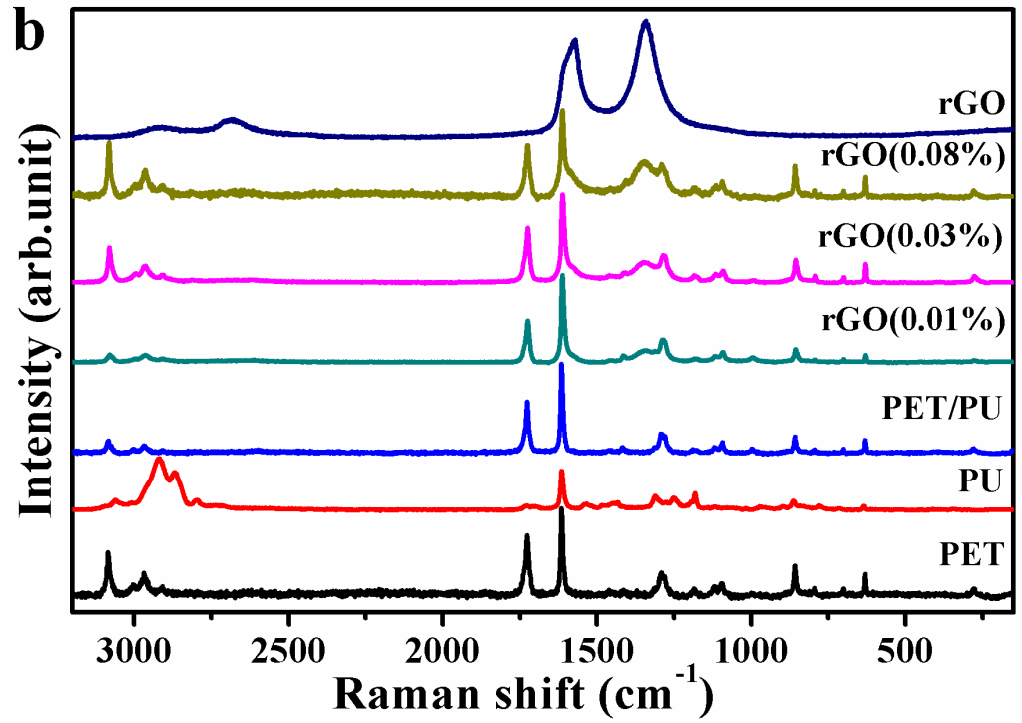

Fig.5(b)

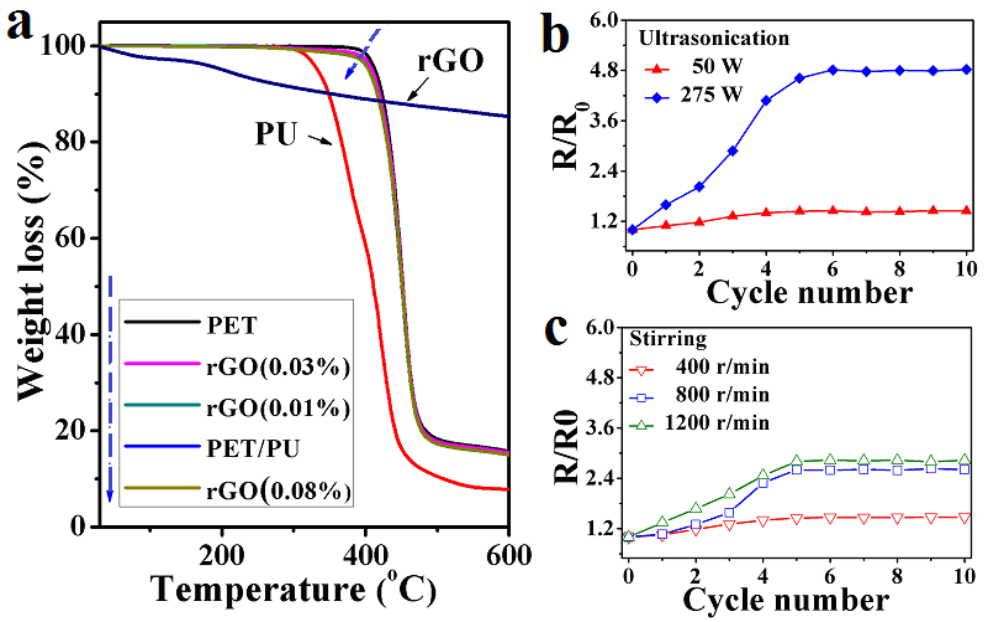

Fi.6

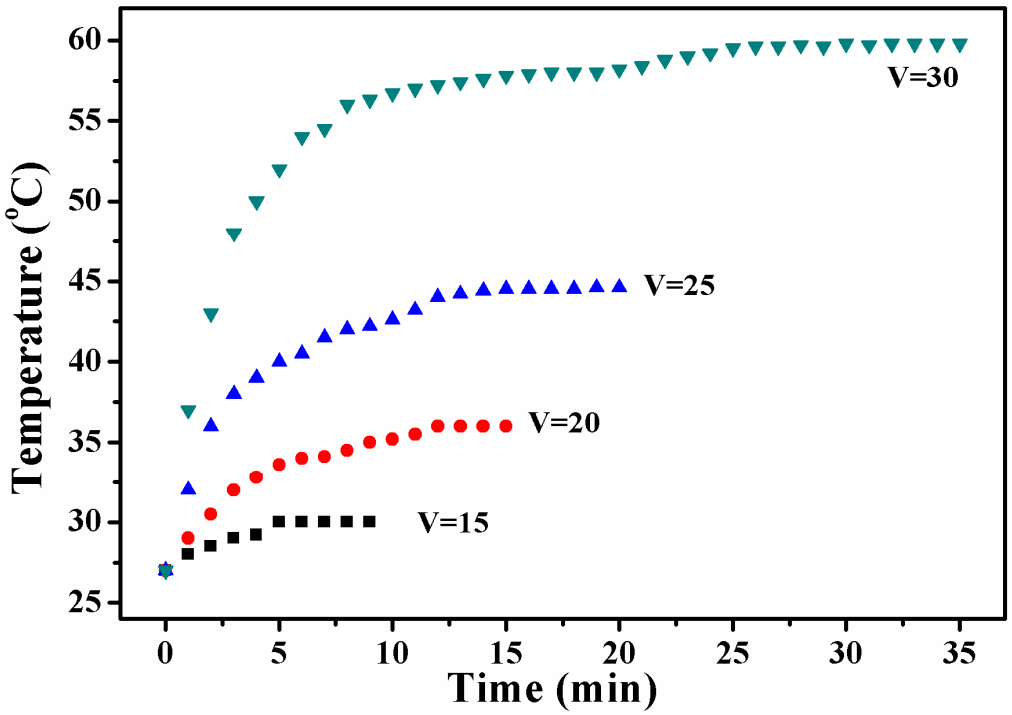

Fig.7

Highlights

▲Utilizing reduced graphene oxides as sheet dyestuffs in aqueous system

▲ Fabricating conductive poly(ethylene terephthalate) nonwoven fabrics through dyeing–like process

▲ Ensuring structural stability by using polyurethane as a middle adhesive layer

▲ Forming a continuous conductive network with low percolation fraction